



HAL
open science

New lanthanide-based coordination polymers with 2,5-dihydroxyterephthalate

Jinzeng Wang, Carole Daiguebonne, Yan Suffren, Stéphane Freslon,
Guillaume Calvez, Kevin Bernot, Olivier Guillou

► **To cite this version:**

Jinzeng Wang, Carole Daiguebonne, Yan Suffren, Stéphane Freslon, Guillaume Calvez, et al.. New lanthanide-based coordination polymers with 2,5-dihydroxyterephthalate. *Inorganica Chimica Acta*, 2021, 527, pp.120594. 10.1016/j.ica.2021.120594 . hal-03370752

HAL Id: hal-03370752

<https://hal.science/hal-03370752v1>

Submitted on 26 Oct 2021

HAL is a multi-disciplinary open access archive for the deposit and dissemination of scientific research documents, whether they are published or not. The documents may come from teaching and research institutions in France or abroad, or from public or private research centers.

L'archive ouverte pluridisciplinaire **HAL**, est destinée au dépôt et à la diffusion de documents scientifiques de niveau recherche, publiés ou non, émanant des établissements d'enseignement et de recherche français ou étrangers, des laboratoires publics ou privés.



Distributed under a Creative Commons Attribution - NonCommercial 4.0 International License

New lanthanide-based coordination polymers with 2,5-dihydroxyterephthalate.

Jinzeng Wang, Carole Daiguebonne, Yan Suffren, Stéphane
Freslon, Guillaume Calvez, Kevin Bernot and Olivier Guillou*

Univ Rennes, INSA Rennes, CNRS UMR 6226 "Institut des Sciences Chimiques de Rennes",
F-35708 Rennes

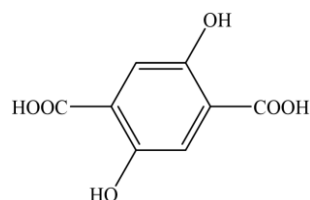
*To whom correspondence should be addressed.

ABSTRACT.

Crystal growths in gel medium of lanthanide-based coordination polymers with 2,5-dihydroxyterephthalate (dhbdc²⁻) as ligand lead to two different crystal structures depending on the lanthanide ion. Lanthanide-based coordination polymers that crystallize in these two structural type have respective chemical formulas $[\text{Ln}_2(\text{dhbdc})_3(\text{H}_2\text{O})_{12}\cdot 6\text{H}_2\text{O}]_\infty$ with $\text{Ln} = \text{La-Nd}$, and $[\text{Ln}_2(\text{dhbdc})_3(\text{H}_2\text{O})_8\cdot 6\text{H}_2\text{O}]_\infty$ with $\text{Ln} = \text{Sm-Yb plus Y}$. Only the Nd-based and the Yb-based coordination polymers exhibit luminescence properties in the near-infrared region.

INTRODUCTION.

For more than twenty years, lanthanide-based coordination polymers have been widely studied because of their remarkable structural diversity¹ as well as because of their unique magnetic and optical properties.²⁻⁸ Lanthanide ions are typical hard Pearson's acids⁹ and present almost no structuring effect because of their shielded valence orbitals.¹⁰ Therefore, derivatives of benzene-poly-carboxylate have been widely used as ligand.¹¹⁻¹² Indeed, their carboxylate functions have good affinity for lanthanide ions and they can act as structuring ligands because of their rigidity and because they can promote π -stacking and H-bond interactions. Among these ligands, benzene-1,4-dicarboxylate (bdc^{2-}) has led to numerous lanthanide-based coordination polymers¹³⁻¹⁴ and some of them exhibit interesting physical properties with actual applicative potential.¹⁵ Our group is concerned for more than twenty years by the quest of new lanthanide-based coordination polymers with interesting structural or physical properties.¹⁶⁻¹⁸ In the frame of this study we have investigated the 2,5-di-hydroxy-terephthalate/lanthanide/ H_2O system (Scheme 1).

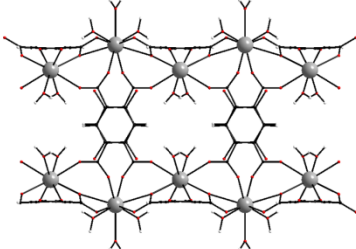
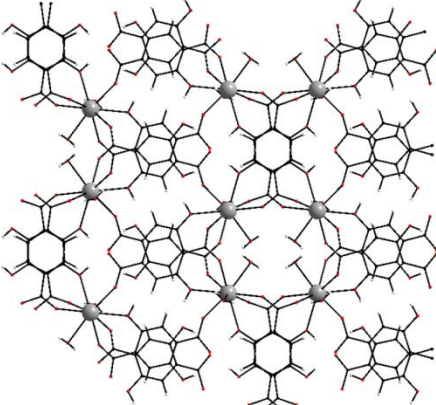
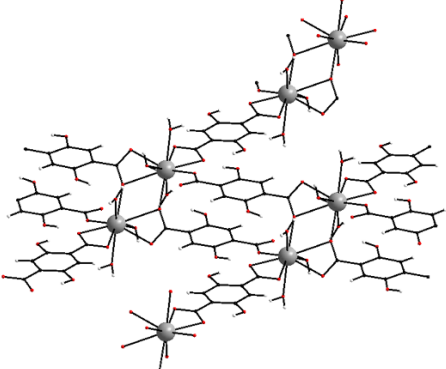


Scheme 1. 2,5-di-hydroxy-benzene-1,4-di-carboxylic acid ($\text{H}_4\text{-dhbdc}$) or 2,5-di-hydroxy-terephthalic acid.

Indeed, the addition of two hydroxy groups, that can be involved in hydrogen-bonds, is expected to play a significant role in the crystal packing. Moreover, this ligand presents two sets of donor oxygen atoms: the two carboxylate functions that can be easily deprotonated (leading to $\text{H}_2\text{-dhbdc}^{2-}$) and the two hydroxyl groups that can be also deprotonated in more severe conditions (leading to the tetra-anionic dbdc^{4-}). Actually, this versatile ligand has been extensively used in combination with 3d transition metal ions as well as alkaline earth metal ions.¹⁹⁻²⁶

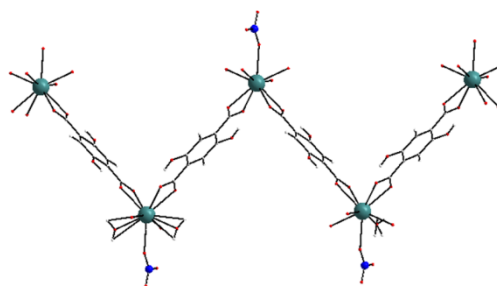
In association with lanthanide ions, this ligand has previously led to several crystalline phases.²⁷⁻³⁰ All of them have been obtained by solvothermal synthesis and consequently both the di-anionic and the tetra-anionic forms of the ligand are present in the chemical formulas. Because the target of our work is to identify compounds suitable for technological transfer only compounds obtained in water are reported in Table 1.

Table 1. Reported structural properties of lanthanide-based coordination polymers with 2,5-di-hydroxy-benzene-1,4-di-carboxylate.

Chemical formula Involved Ln ³⁺ Reference CCDC n° Framework dimension	System Space group Cell parameters	Projection view
$[\text{Ln}_2(\text{dhbdc})(\text{H}_2\text{-dhbdc})(\text{H}_2\text{O})_5 \cdot 2\text{H}_2\text{O}]_\infty$ Ln = Gd Reference 28 CCDC n° 748734 2D	Monoclinic <i>P2/c</i> (n°13) $a = 8.9065(2) \text{ \AA}$ $b = 15.0925(3) \text{ \AA}$ $c = 8.5028(2) \text{ \AA}$ $\beta = 96260(1)^\circ$ $V = 1136.14(4) \text{ \AA}^3$	
$[\text{Ln}_2(\text{H}_2\text{-dhbdc})_3(\text{H}_2\text{O})_4]_\infty$ Ln = La, Pr Reference 27 CCDC n° 879608 3D	Monoclinic <i>C2/c</i> (n°15) $a = 29.844(7) \text{ \AA}$ $b = 13.113(3) \text{ \AA}$ $c = 6.7951(16) \text{ \AA}$ $\beta = 101.574(3)^\circ$ $V = 2605.1(11) \text{ \AA}^3$	
$[\text{Ln}_2(\text{H}_2\text{-dhbdc})_3(\text{H}_2\text{O})_6 \cdot 2\text{H}_2\text{O}]_\infty$ Ln = Nd Reference 27 CCDC n° 879609 2D	Triclinic <i>P1̄</i> (n°2) $a = 8.1061(15) \text{ \AA}$ $b = 9.9258(18) \text{ \AA}$ $c = 10.6687(19) \text{ \AA}$ $\alpha = 76.061(2)^\circ$ $\beta = 74.789(2)^\circ$ $\gamma = 74.686(2)^\circ$ $V = 785.2(2) \text{ \AA}^3$	

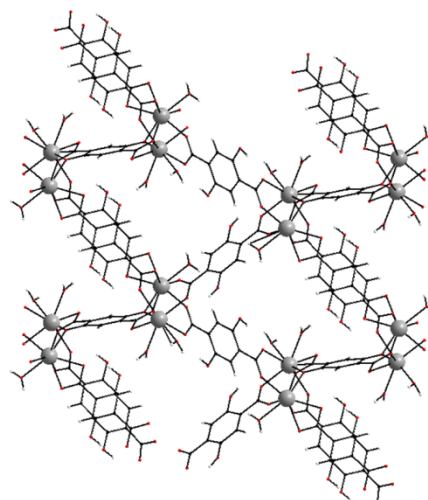
$[\text{Ln}(\text{H}_2\text{-dihbdc})(\text{NO}_3)(\text{H}_2\text{O})_4 \cdot 2\text{H}_2\text{O}]_\infty$
Ln = **Eu**
Reference 27
CCDC n° 879610
1D

Orthorhombic
 $Pnma$ ($n^{\circ}62$)
 $a = 15.5221(1) \text{ \AA}$
 $b = 15.5219(6) \text{ \AA}$
 $c = 6.4783(2) \text{ \AA}$
 $V = 1560.81(8) \text{ \AA}^3$



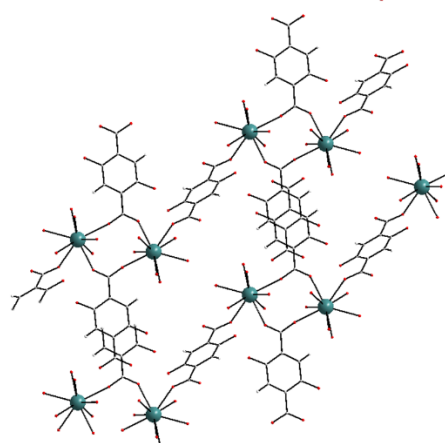
$[\text{Ln}_2(\text{H}_2\text{-dihbdc})(\text{dihbdc})(\text{H}_2\text{O})_3 \cdot 4\text{H}_2\text{O}]_\infty$
Ln = Gd, **Dy**
Reference 27
CCDC n° 879612
3D

Triclinic
 $P\bar{1}$ ($n^{\circ}2$)
 $a = 7.3494(4) \text{ \AA}$
 $b = 11.4750(6) \text{ \AA}$
 $c = 16.1852(8) \text{ \AA}$
 $\alpha = 78.7990(10)^{\circ}$
 $\beta = 82.4830(10)^{\circ}$
 $\gamma = 79.9550(10)^{\circ}$
 $V = 1311.79(12) \text{ \AA}^3$



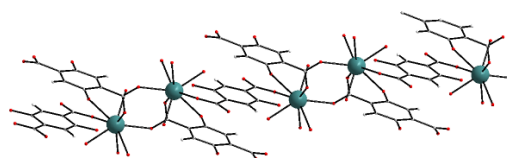
$[\text{Ln}_2(\text{H}_2\text{-dihbdc})_3(\text{H}_2\text{O})_{12} \cdot 6\text{H}_2\text{O}]_\infty$
Ln = **La**-Nd
Reference: This work
CCDC n° 1913155
2D

Triclinic
 $P\bar{1}$ ($n^{\circ}2$)
 $a = 6.9079(8) \text{ \AA}$
 $b = 11.8793(12) \text{ \AA}$
 $c = 13.1925(14) \text{ \AA}$
 $\alpha = 70.602(3)^{\circ}$
 $\beta = 78.415(3)^{\circ}$
 $\gamma = 78.737(3)^{\circ}$
 $V = 990.60(19) \text{ \AA}^3$



$[\text{Ln}_2(\text{H}_2\text{-dihbdc})_3(\text{H}_2\text{O})_8 \cdot 6\text{H}_2\text{O}]_\infty$
Ln = Sm-Yb plus **Y**
Reference: This work (**Er**) and 29
(**Tb**)
CCDC n° 1913156 and 1503699
1D

Triclinic
 $P\bar{1}$ ($n^{\circ}2$)
 $a = 9.6236(12) \text{ \AA}$
 $b = 10.1882(13) \text{ \AA}$
 $c = 11.6786(13) \text{ \AA}$
 $\alpha = 113.728(4)^{\circ}$
 $\beta = 100.914(4)^{\circ}$
 $\gamma = 105.642(4)^{\circ}$
 $V = 950.08(21) \text{ \AA}^3$



In bold, the lanthanide ion involved in the solved crystal structure

In the following, the syntheses and the crystal structures of two series of lanthanide-based coordination polymers are described as well as the luminescence properties of the Nd- and Yb-derivatives.

EXPERIMENTAL SECTION.

Lanthanide oxides (4N) were purchased from Ampere and their chloride salts were prepared according to established procedures.³¹ 2,5-di-hydroxy-benzene-1,4-di-carboxylic acid (H₄-dhbdc) (>98%) was purchased from TCI and used without further purification. Tetramethylorthosilicate (TMOS) was purchased from Accros and jellified according to previously published procedures.³²⁻³³

Synthesis of Na₂(H₂-dhbdc)·0.5H₂O

To a suspension in water of H₄-dhbdc, a stoichiometric amount of sodium hydroxide was added leading to a clear solution that was evaporated to dryness. The obtained solid was then dissolved in ethanol and refluxed for one hour. Addition of ethoxyethane provokes precipitation. The obtained brown precipitate was filtered, washed with ethoxyethane and dry in air. The yield was about 90%. C₈H₅Na₂O_{6.5} (MW = 251 g.mol⁻¹) Analysis: (calc.) found: C (38.2%) 38.5%; H (2.0%) 2.2%; O (41.4%) 41.3%; Na (8.3%) 8.0 %. Thermogravimetric analysis confirms that this salt is hemi-hydrated. Its X-ray powder diffraction diagram is reported in figure S1.

Despite great efforts, we did not succeed in obtaining single crystals suitable for X-ray crystal structure determination. However, it can be noticed that during these attempts we obtained single crystals of a mono-deprotonated phase with chemical formula [Na(H₃-dhbdc)(H₂O)₂]_∞. It crystallizes in the monoclinic system, space group *P*2₁/*n* (n°14) with the following cell parameters: *a* = 8.8788(6) Å, *b* = 6.8920(5) Å, *c* = 16.2174(12) Å, β = 96.259(3)°, *V* = 986.47(12) Å³ and *Z* = 4. This crystal structure is described in Supporting Information (Figures S2 and S3 and Table S1).

Crystal growth of the lanthanide-based coordination polymers.

Single crystals suitable for X-ray diffraction crystal structure determination were obtained by slow diffusion of the reactants (a lanthanide chloride aqueous solution in one hand and a $\text{Na}_2(\text{H}_2\text{-dhbc})\cdot 0.5\text{H}_2\text{O}$ aqueous solution in the other hand) through a TMOS gel (7.5% in weight) in U-shaped tubes.³⁴ After some weeks, brown rod-like single crystals were collected. Coordination polymers present two different crystal structures depending on the involved lanthanide ion: For lanthanide ions comprised between lanthanum and neodymium, they have general chemical formula $[\text{Ln}_2(\text{H}_2\text{-dhbdc})_3(\text{H}_2\text{O})_{12}\cdot 6\text{H}_2\text{O}]_\infty$ and $[\text{Ln}_2(\text{H}_2\text{-dhbdc})_3(\text{H}_2\text{O})_8\cdot 6\text{H}_2\text{O}]_\infty$ for heavier lanthanide ions and yttrium.

Synthesis of the lanthanide-based coordination polymers as microcrystalline powders.

An aqueous solution of a lanthanide chloride ($\text{Ln} = \text{La-Yb plus Y}$) (0.2 mmol in 5 mL of deionized water) was added to an aqueous solution of the di-sodium salt of 2,5-di-hydroxy-benzene-1,4-di-carboxylic acid (0.3 mmol in 5 mL of deionized water) at room temperature. The mixture was stirred over 72h in order to insure complete precipitation. Then, the brown precipitate was filtered, rinsed with water and dried in air. The yield was about 90%. The obtained lanthanide-based coordination polymers can be shared in two series of isostructural compounds depending on the lanthanide ion on the basis of their X-ray powder diffraction diagrams (Figures S4 and S5). Elemental analyses are listed in Table S2.

X-ray diffraction

Powder X-ray diffraction diagrams were collected with a Panalytical X'Pert Pro diffractometer equipped with a X'Celerator detector. Typical recording conditions were: 45 kV,

40 mA, Cu K_{α} radiation ($\lambda = 1.542 \text{ \AA}$), θ/θ mode. Simulated patterns from crystal structure were produced with PowderCell and WinPLOTR programs.³⁵⁻³⁷

Crystal structures of the two series of coordination polymers have been solved based on the lanthanum- and erbium-derivatives, respectively. Single crystals were mounted on a Bruker D8 Venture diffractometer. Crystal data collection were performed at 150 K with Mo K_{α} radiation ($\lambda = 0.70713 \text{ \AA}$). Crystal structures were solved, using SIR 97,³⁸ by direct methods. They were refined, using SHELX-2017³⁹⁻⁴⁰ with the aid of WINGX program.⁴¹⁻⁴² All non-hydrogen atoms were refined anisotropically. Hydrogen atoms that have been located were located at ideal positions. Absorption corrections were performed using the facilities of WINGX program.⁴³ Selected crystal and final structure refinement data are gathered in Table 2. It can be noticed that some residual density peaks are present in the vicinity of the Er^{3+} ion in the second structural family. These peaks are likely due to an imperfect absorption correction. Despite great efforts, it has not been possible to remove them. Full details of the crystal structures have been deposited with the Cambridge Crystallographic Data Centers under the depositary numbers CCDC-1913155 for $[\text{La}_2(\text{H}_2\text{-dhbdc})_3(\text{H}_2\text{O})_{12}\cdot 6\text{H}_2\text{O}]_{\infty}$ and CCDC-1913156 for $[\text{Er}_2(\text{H}_2\text{-dhbdc})_3(\text{H}_2\text{O})_8\cdot 6\text{H}_2\text{O}]_{\infty}$.

Table 2. Crystallographic data for $[\text{La}_2(\text{H}_2\text{-dihbdc})_3(\text{H}_2\text{O})_{12}\cdot 6\text{H}_2\text{O}]_\infty$ and $[\text{Er}_2(\text{H}_2\text{-dihbdc})_3(\text{H}_2\text{O})_8\cdot 6\text{H}_2\text{O}]_\infty$		
	$[\text{La}_2(\text{H}_2\text{-dihbdc})_3(\text{H}_2\text{O})_{12}\cdot 6\text{H}_2\text{O}]_\infty$	$[\text{Er}_2(\text{H}_2\text{-dihbdc})_3(\text{H}_2\text{O})_8\cdot 6\text{H}_2\text{O}]_\infty$
Chemical formula	$\text{C}_{12}\text{H}_{24}\text{LaO}_{18}$	$\text{C}_{12}\text{H}_{20}\text{ErO}_{16}$
System	Triclinic	Triclinic
Space group (n°)	$\text{P}\bar{1}$ ($n^\circ 2$)	$\text{P}\bar{1}$ ($n^\circ 2$)
Formula weight ($\text{g}\cdot\text{mol}^{-1}$)	595.22	587.54
a (\AA)	6.9079(8)	9.6236(12)
b (\AA)	11.8793(12)	10.1882(13)
c (\AA)	13.1925(14)	11.6786(13)
α ($^\circ$)	70.602(3)	113.728(4)
β ($^\circ$)	78.415(3)	100.914(4)
γ ($^\circ$)	78.737(3)	105.642(4)
V (\AA^3)	990.60(19)	950.1(2)
Z	2	2
θ range ($^\circ$)	2.822-27.505	2.258-27.608
D_{calc} ($\text{g}\cdot\text{cm}^{-3}$)	1.996	2.054
R	0.0146	0.0272
R_w	0.0386	0.0669
GoF	1.108	1.216
$\Delta\rho$ min/max ($\text{e}\cdot\text{\AA}^{-3}$)	-0.68/0.39	-1.58/2.10
CCDC number	1913155	1913156

Thermal analyses.

Thermal analyses have been performed using a Perkin Elmer Pyris Diamond TGA/TDA, between 25°C and 950°C in platinum crucibles under N_2 atmosphere.

Optical measurements.

Solid-state emission and excitation spectra have been measured on a Horiba Jobin-Yvon Fluorolog III fluorescence spectrometer equipped with a Xe lamp 450 W, an UV-Vis photomultiplier (Hamamatsu R928, sensitivity 190 - 860 nm) and an IR-photodiode cooled by liquid nitrogen (InGaAs, sensitivity 800 – 1600 nm). The emission/excitation spectra recordings were realized on powder samples pasted on copper plates with silver glue. The emission from Gd-microcrystalline powders has been also measured at variable temperature (77 K – 293 K): the sample pasted on copper plate was introduced in an OptistatCF liquid nitrogen cooled cryostat from Oxford Instruments. Appropriate filters were used to remove the

residual excitation laser light, the Rayleigh scattered light and associated harmonics from spectra. All spectra were corrected for the instrumental response function.

RESULTS AND DISCUSSION

Reaction in water of lanthanide chloride with the di-sodium salt of 2,5-di-hydroxy-benzene-1,4-di-carboxylic acid lead to two series of iso-structural coordination polymers. The first family gathers the compounds obtained with one of the lightest lanthanide ion ($\text{Ln} = \text{La-Nd}$) and have general chemical formula $[\text{Ln}_2(\text{H}_2\text{-dihbdc})_3(\text{H}_2\text{O})_{12}\cdot 6\text{H}_2\text{O}]_\infty$. The second family gathers the compounds that have been obtained with one of the heavier lanthanide ions ($\text{Ln} = \text{Sm-Yb}$) plus yttrium and have general chemical formula $[\text{Er}_2(\text{H}_2\text{-dihbdc})_3(\text{H}_2\text{O})_8\cdot 6\text{H}_2\text{O}]_\infty$.

Crystal structure of $[\text{Ln}_2(\text{H}_2\text{-dihbdc})_3(\text{H}_2\text{O})_{12}\cdot 6\text{H}_2\text{O}]_\infty$ with $\text{Ln} = \text{La-Nd}$.

These compounds crystallize in the triclinic system, space group $P\bar{1}$ ($n^{\circ}2$). Their crystal structure has been solved on the basis of the lanthanum derivative. Isostructurality of the others members of the family has been assumed on the basis of their powder X-ray diffraction patterns (Figure S4). There is only one independent La^{3+} ion in this crystal structure. It is nine-coordinated by nine oxygen atoms that form a slightly distorted capped square antiprism. Six out of the nine oxygen atoms belong to six coordination water molecules and the remaining three arise from three different ligands (Figure 1).

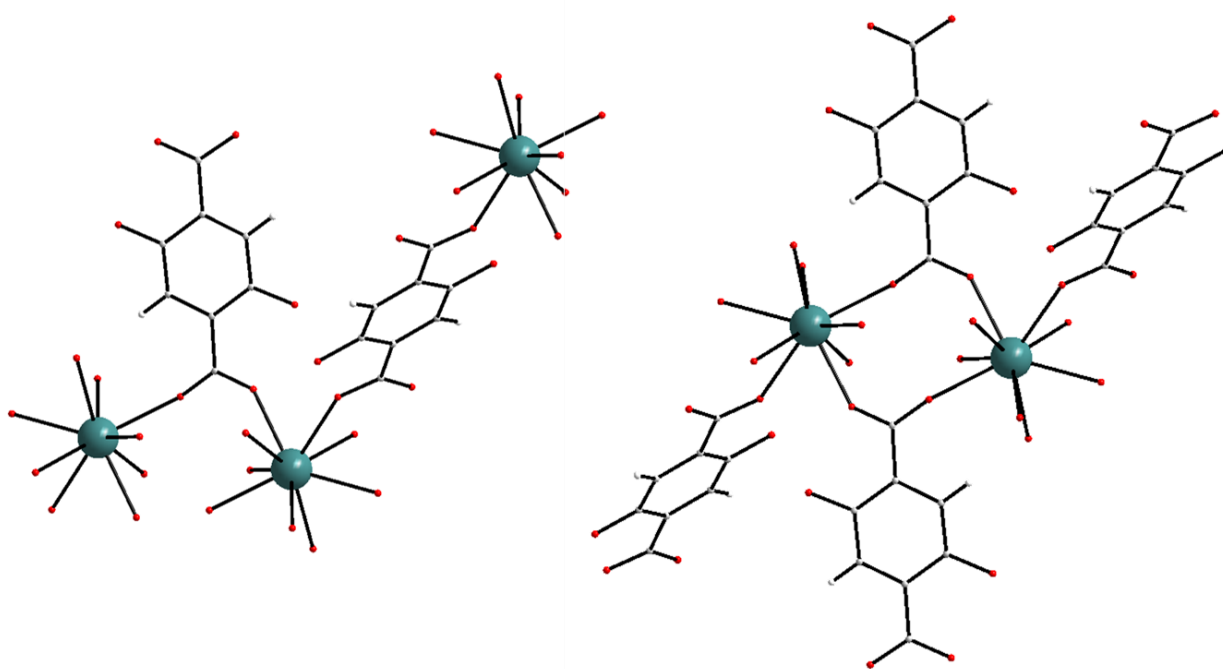


Figure 1. Binding modes of the ligands (left) and lanthanum ion neighborhood in $[\text{La}_2(\text{H}_2\text{-dhbdc})_3(\text{H}_2\text{O})_{12}\cdot 6\text{H}_2\text{O}]_\infty$.

There are two crystallographically independent ligands. Both are twice deprotonated (dhbdc^{2-}) and both connect two La^{3+} ions (Figure 1 Left). The first one is centered on an inversion center. It binds two La^{3+} ions in unidentate way via two oxygen atoms of one of its carboxylate function, which leads to dimeric units (Figure 1). The inter-metallic distance in these dimeric units is $5.5742(7)$ Å. The second carboxylate function is non-bonding. The second ligand connects these dimeric units to each other via its two carboxylate functions leading to a molecular chain-like motif (Figure 2). The shortest intermetallic distance between La^{3+} ions that belong to neighboring dimeric units is $12.3613(10)$ Å.

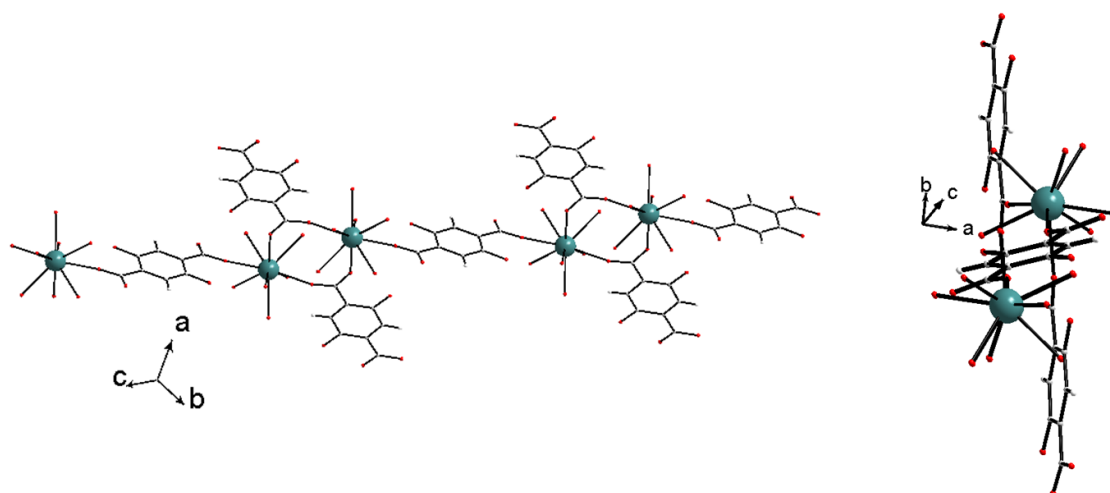


Figure 2. Projection views of the molecular chain like motif of $[\text{La}_2(\text{H}_2\text{-dhbdc})_3(\text{H}_2\text{O})_{12}\cdot 6\text{H}_2\text{O}]_\infty$.

In addition to the twelve coordination water molecules, there are six crystallization water molecules per formula unit as confirmed by the thermal analyses (Figure S6). The stability of the crystal packing is insured by a complex network of hydrogen bonds as well as by π -stacking interactions (Figure 3).

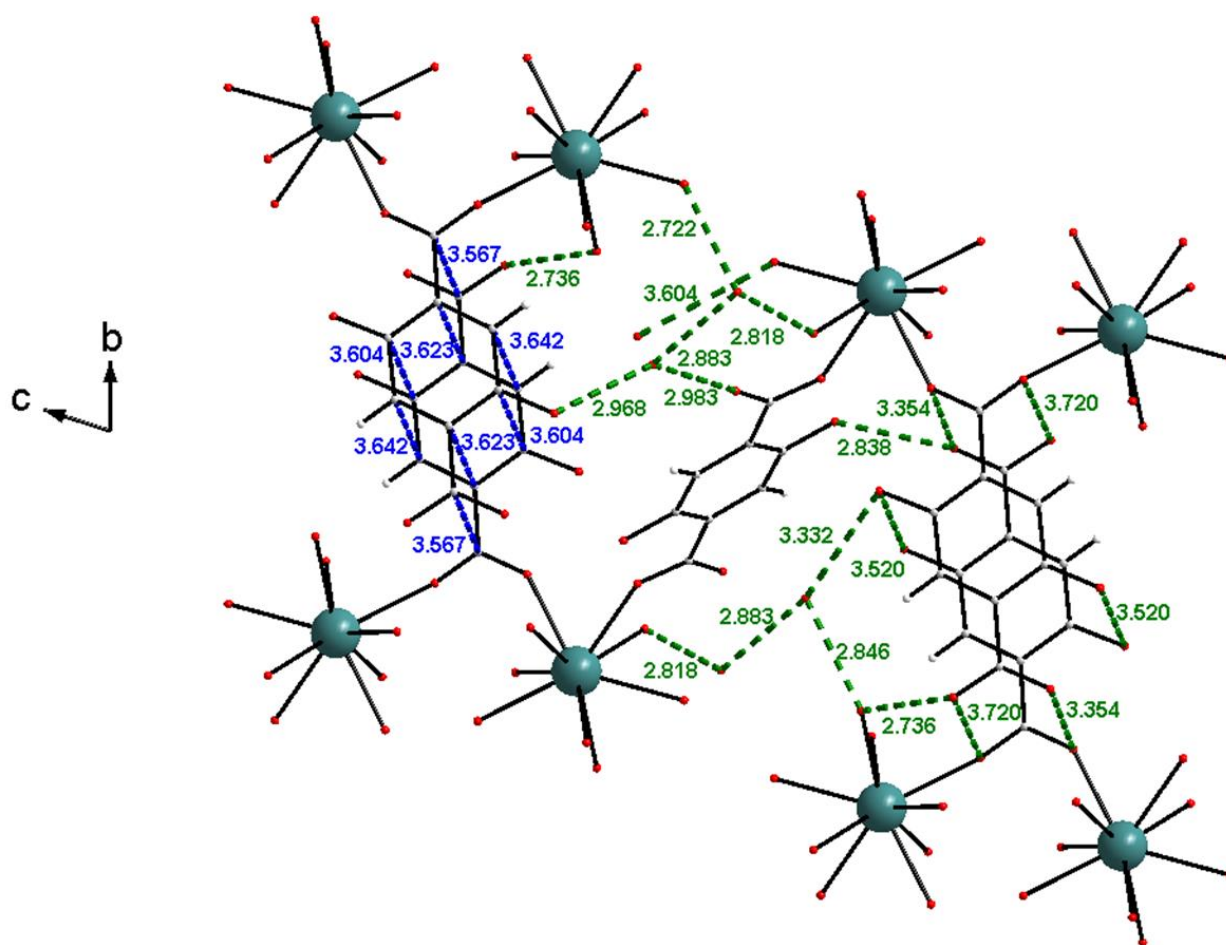


Figure 3. Projection view, along the a -axis of $[\text{La}_2(\text{H}_2\text{-dhbdc})_3(\text{H}_2\text{O})_{12}\cdot 6\text{H}_2\text{O}]_\infty$. Green broken-lines stand for H-bonds and blue ones for π -stacking interactions.

Crystal structure of $[\text{Ln}_2(\text{H}_2\text{-dhbdc})_3(\text{H}_2\text{O})_8\cdot 6\text{H}_2\text{O}]_\infty$ with $\text{Ln} = \text{Sm-Yb}$ plus Y .

These compounds are all iso-structural (Figure S5). The crystal structure has been solved on the basis of the Er-derivative. It crystallizes in the triclinic system, space group $P\bar{1}$ ($n^{\circ}2$). It can be noticed that the crystal structure of the Tb-derivative has previously been reported by Anderson *et al.* in 2017.²⁹ In this study, the Tb-derivative was obtained as a metastable kinetic phase by post-synthetic solvent exchange from $[\text{Tb}_2(\text{H}_2\text{-dhbdc})_3(\text{DMF})_4\cdot 2\text{DMF}]_\infty$.³⁰

There is only one crystallographically independent Er^{3+} ion in the asymmetric unit. It is eight coordinated by four oxygen atoms from coordination water molecules, three monodentate oxygen atoms from three carboxylate functions from three different ligands and one oxygen

atom that belongs to a hydroxo group (Figure 4). Its coordination polyhedron is best described as a bi-augmented trigonal prism.

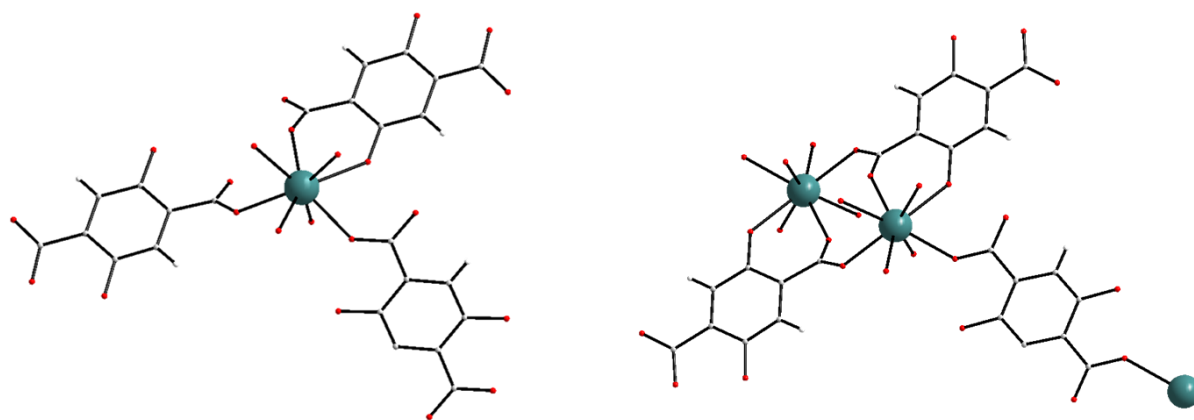


Figure 4. Er^{3+} neighborhood (left) and ligands coordination modes (right) in $[\text{Er}_2(\text{H}_2\text{-dhbdc})_3(\text{H}_2\text{O})_8 \cdot 6\text{H}_2\text{O}]_\infty$.

There are two different ligands in the crystal structure. Two ligands of the first type strongly connect two Er^{3+} ions to each other: one Er^{3+} ion is bound by a monodentate oxygen of a carboxylate function while the second Er^{3+} ion is bound by the second oxygen atom of this carboxylate function and by an oxygen atom of a hydroxo group that belongs to the same ligand. The intermetallic distance in these dimeric units is $5.0104(5) \text{ \AA}$. The second ligand connects these dimeric units via monodentate oxygen atoms of its carboxylate functions. This leads to molecular chain-like motifs (Figure 5). The shortest distance between Er^{3+} ions that belong to adjacent dimeric units in the same chain-like molecular motif is $11.1490(11) \text{ \AA}$. The shortest intermetallic distance between lanthanide ions that belong to adjacent chain-like molecular motifs is $7.7436(10) \text{ \AA}$. There are eight coordination water molecules and six crystallization water molecules per formula units as confirmed by thermal analyses (Figure S7). These water molecules are involved in a complex hydrogen-bonds network that insures the stability of the crystal packing.

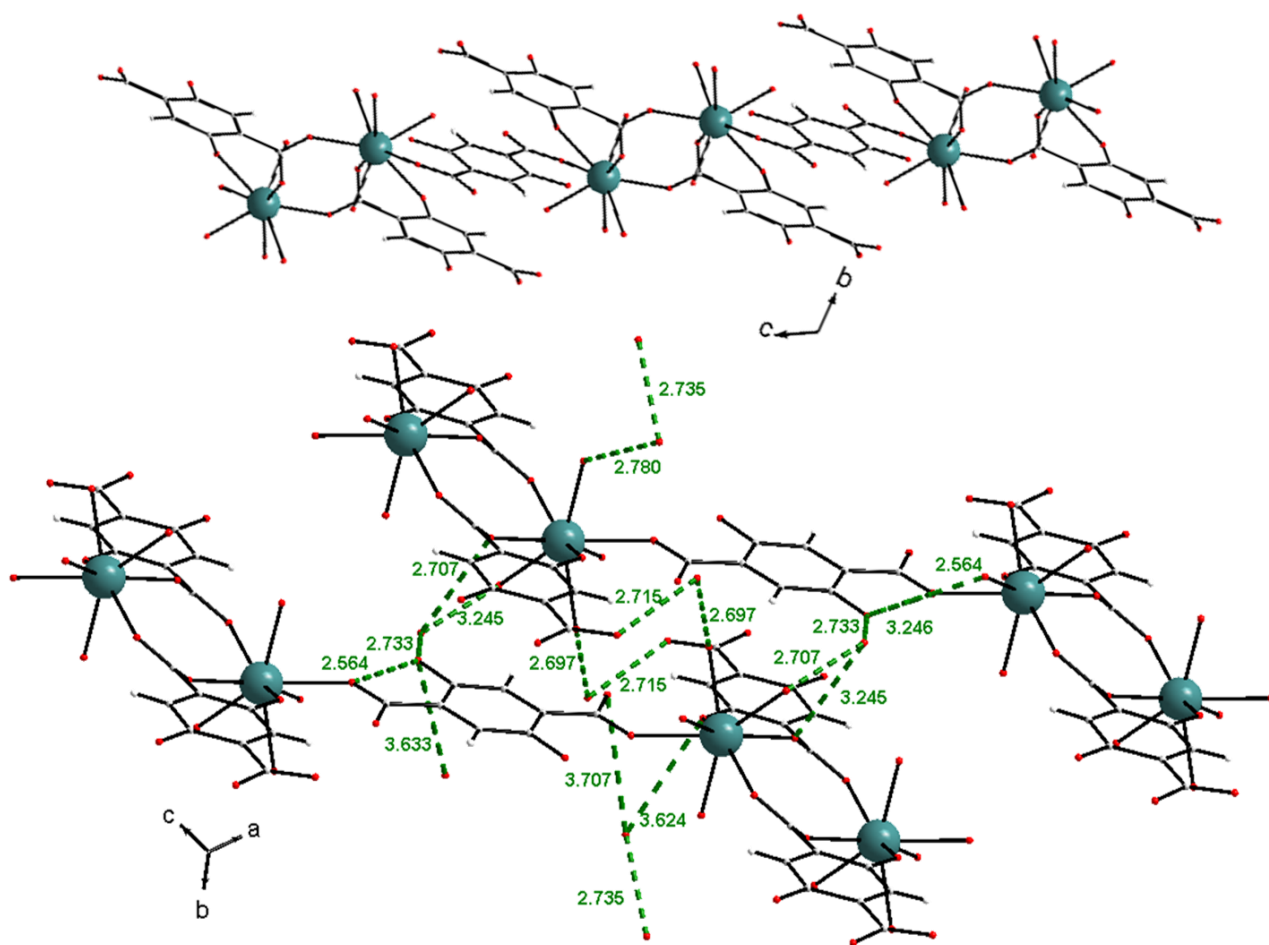


Figure 5. Chain-like molecular motif (top) and hydrogen-bonds network (bottom) in $[\text{Er}_2(\text{H}_2\text{-dhbdc})_3(\text{H}_2\text{O})_8 \cdot 6\text{H}_2\text{O}]_\infty$. Hydrogen-bonds are drawn as green broken-lines.

Luminescent properties of $[\text{Ln}_2(\text{H}_2\text{-dhbdc})_3(\text{H}_2\text{O})_{12} \cdot 6\text{H}_2\text{O}]_\infty$ with Ln = La-Nd

Excitation spectra that have been recorded for the La- and the Nd-derivatives show a broad excitation band that can be attributed to the ligand $^1\pi^*/^3\pi^* \leftarrow ^1\pi$ transitions. As expected, because of the two OH groups, this broad band is red-shifted in comparison with what has been observed for other terephthalate derivatives.⁴⁴⁻⁴⁶ Its maximum intensity is observed for about $\lambda_{\text{exc}} = 328$ nm but it extends as far as 450 nm (Figures 6 and 7). The emission spectrum of the lanthanum derivative shows a broad band that extends from 400 nm to 800 nm, which induces bright yellow emission (Figure 6). It is noticeable that this phosphorescence band is unusually intense at room temperature. It has been measured from room temperature to 77 K (Figure S8).

This measurements show that the luminescence band is blue-shifted and more intense as the temperature decreases.

Emission spectra of the Nd-based compound have been measured for λ_{exc} equal to 330 nm (maximum of the excitation band), 400 nm (second extremum of the excitation band) and 581 nm (${}^4G_{7/2-5/2} \leftarrow {}^4I_{9/2}$ excitation peak of the Nd^{3+} ion) (Figure 7). These three emission spectra confirm that the ligand present an efficient antenna effect⁴⁷ toward the Nd^{3+} ion. The ${}^4F_{3/2} \rightarrow {}^4I_{9/2}$, ${}^4I_{11/2}$ and ${}^4I_{13/2}$ transitions are observed at 890, 1056 and 1335 nm, respectively. Indeed, the emission intensity under excitation of the ligand is much stronger than that observed under direct excitation of the lanthanide ion.

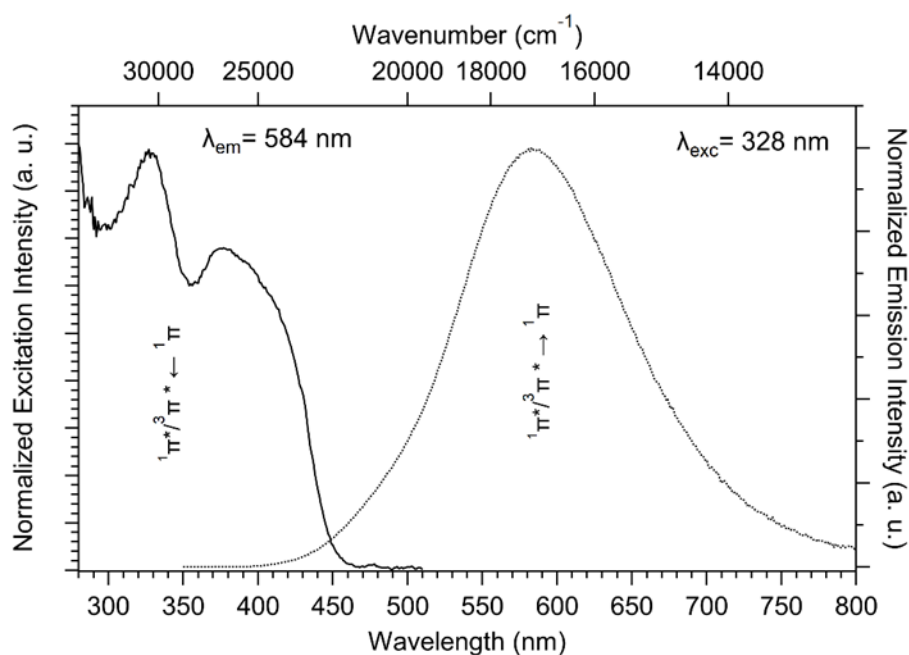


Figure 6. Room temperature solid-state excitation ($\lambda_{\text{em}} = 584$ nm) and emission ($\lambda_{\text{exc}} = 328$ nm) spectra of $[\text{La}_2(\text{H}_2\text{-dhbdc})_3(\text{H}_2\text{O})_{12} \cdot 6\text{H}_2\text{O}]_\infty$.

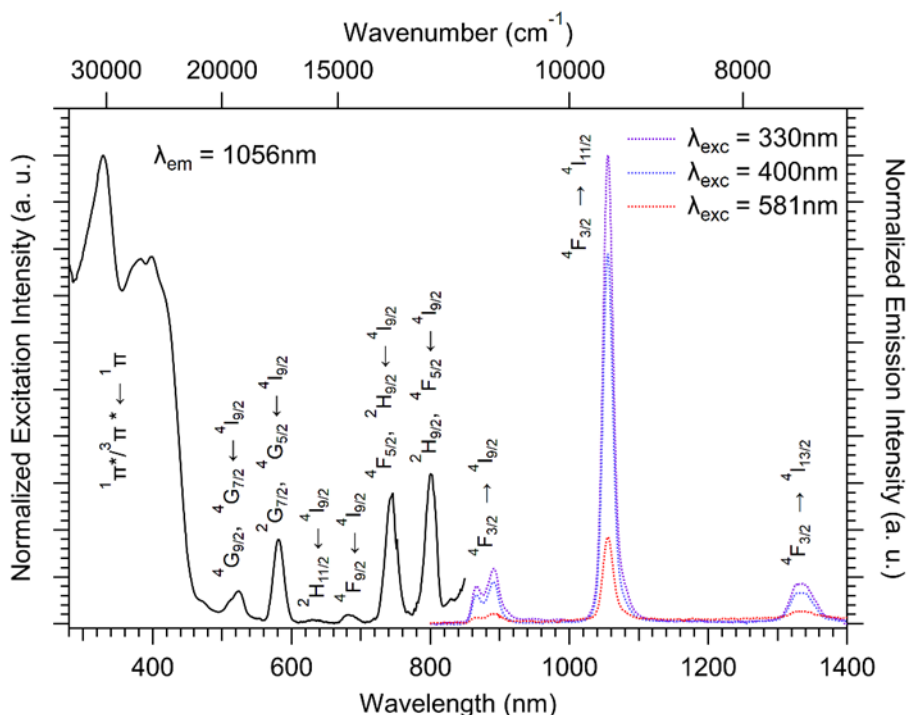


Figure 7. Room temperature solid-state excitation ($\lambda_{em} = 1056$ nm, dark curve) and emission ($\lambda_{exc} = 330$ nm, 400 nm and 581 nm for dotted purple, blue and red curves, respectively) spectra of $[\text{Nd}_2(\text{H}_2\text{-dhbdc})_3(\text{H}_2\text{O})_{12}\cdot 6\text{H}_2\text{O}]_\infty$.

The Pr^{3+} derivative shows no luminescence because emissive excited states of the Pr^{3+} ion are higher in energy than the donor excited states of the ligand.⁴⁸

Luminescent properties of $[\text{Ln}_2(\text{H}_2\text{-dhbdc})_3(\text{H}_2\text{O})_8\cdot 6\text{H}_2\text{O}]_\infty$ with Ln = Sm-Yb plus Y.

The room temperature absorption spectrum of the Gd-derivative has been recorded (Figure S9). It shows that the first excited singlet state of the ligand is about 450 nm (22220 cm^{-1})⁴⁹ that is lower than the absorption peaks of the lanthanide ions that emit in the visible region (Sm^{3+} , Tb^{3+} , Eu^{3+} and Dy^{3+}).⁵⁰ Therefore, neither direct excitation of the lanthanide ion nor excitation via an antenna effect is possible and no luminescence is observed for any of these derivatives. On the opposite, the Yb^{3+} emitting level ($^2\text{F}_{5/2}$) energy is 10180 cm^{-1} and therefore the Yb^{3+} -derivative presents a luminescence in the NIR domain (Figure 8)⁴⁸. Its emission spectrum (under ligand excitation at 330 nm and 400 nm) shows only one peak centered at 978 nm that can be attributed to the $^2\text{F}_{5/2} \rightarrow ^2\text{F}_{7/2}$ transition.

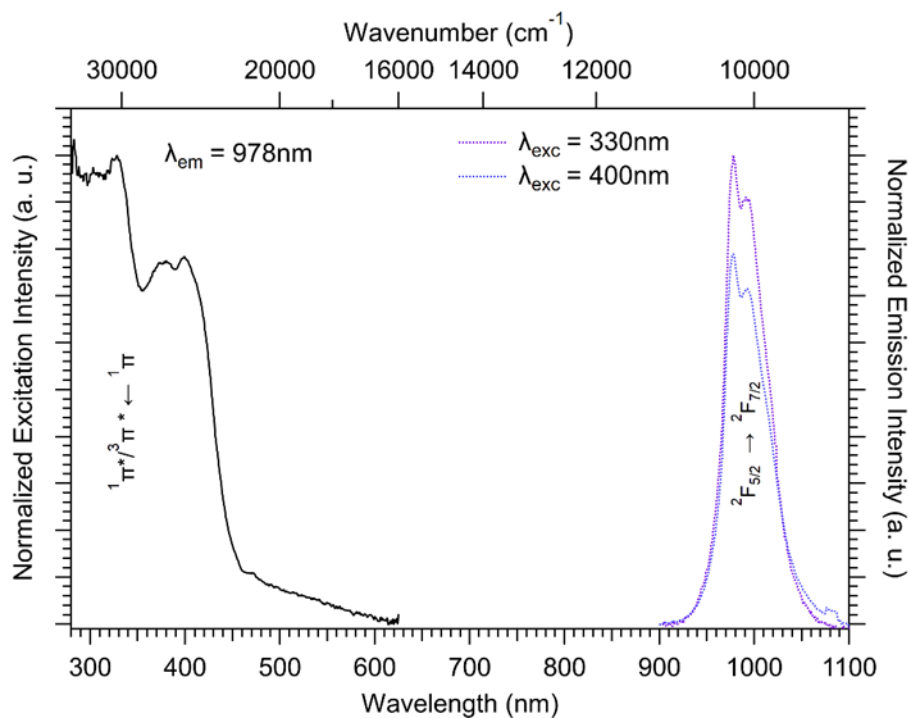


Figure 8. Room temperature solid-state excitation spectra of $[\text{Yb}_2(\text{H}_2\text{-dhbdc})_3(\text{H}_2\text{O})_8 \cdot 6\text{H}_2\text{O}]_\infty$.

CONCLUSION AND OUTLOOK.

Two new series of lanthanide-based coordination polymers with 2,5-di-hydroxy-benzene-1,4-di-carboxylate ligand have been structurally described. Two compounds that belong to these families ($[\text{Nd}_2(\text{H}_2\text{-dhbdc})_3(\text{H}_2\text{O})_{12} \cdot 6\text{H}_2\text{O}]_\infty$ and $[\text{Yb}_2(\text{H}_2\text{-dhbdc})_3(\text{H}_2\text{O})_8 \cdot 6\text{H}_2\text{O}]_\infty$) present interesting luminescent properties in the NIR domain. The coordination polymers based on lanthanide ions that usually exhibit luminescence in the visible domain present no luminescence because of the red-shift of the absorption band of the ligand.

ACKNOWLEDGEMENTS.

The Chinese Scholarship Council is acknowledged for its financial support in the frame of the Chinese-INSA/UT network

SUPPORTING INFORMATION

Crystal structure description of $[\text{Na}(\text{H}_3\text{-dihbdc})(\text{H}_2\text{O})_2]_\infty$; Experimental powder X-ray diffraction diagrams of $\text{Na}_2(\text{H}_2\text{-dihbdc})\cdot 0.5\text{H}_2\text{O}$, $[\text{Ln}_2(\text{H}_2\text{-dihbdc})_3(\text{H}_2\text{O})_{12}\cdot 6\text{H}_2\text{O}]_\infty$ ($\text{Ln} = \text{La-Nd}$) and $[\text{Ln}_2(\text{H}_2\text{-dihbdc})_3(\text{H}_2\text{O})_8\cdot 6\text{H}_2\text{O}]_\infty$ ($\text{Ln} = \text{Sm-Lu plus Y}$); Elemental analyses of the micro-crystalline powders of the lanthanide-based coordination polymers; Thermal analyses of $[\text{La}_2(\text{H}_2\text{-dihbdc})_3(\text{H}_2\text{O})_{12}\cdot 6\text{H}_2\text{O}]_\infty$ and of $[\text{Er}_2(\text{H}_2\text{-dihbdc})_3(\text{H}_2\text{O})_8\cdot 6\text{H}_2\text{O}]_\infty$; Normalized emission intensity *versus* temperature of $[\text{La}_2(\text{H}_2\text{-dihbdc})_3(\text{H}_2\text{O})_{12}\cdot 6\text{H}_2\text{O}]_\infty$; Room temperature solid-state absorption spectrum of $[\text{Gd}_2(\text{H}_2\text{-dihbdc})_3(\text{H}_2\text{O})_8\cdot 6\text{H}_2\text{O}]_\infty$.

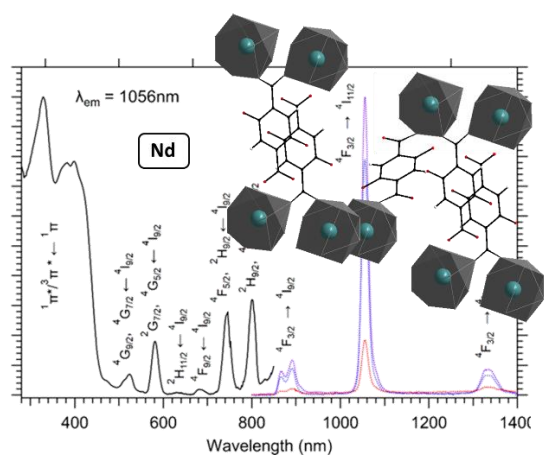
REFERENCES

1. F. Saraci; V. Quezada-Novoa; P. R. Donnarumma; A. J. Howarth, Rare-earth metal–organic frameworks: from structure to applications. *Chem. Soc. Rev.* 2020, **49**, 7949-7077.
2. Y. Cui; J. Zhang; H. He; G. Qian, Photonic functional metal–organic frameworks. *Chem. Soc. Rev.* 2018, **47**, 5740-5785.
3. Y. Cui; B. Li; H. He; W. Zhou; B. Chen; G. Qian, Metal-organic frameworks as platforms for functional materials. *Accounts Chem. Res.* 2016, **49**, 483-493.
4. Y. Cui; J. Zhang; B. Chen; G. Qian, Lanthanide Metal-Organic Frameworks for Luminescent Applications. *Handbook on the Physics and Chemistry of Rare Earths* 2016, **50**, 243-268.
5. R. Sessoli; K. Bernot, Lanthanides in extended molecular networks. In *Molecular magnetism*, Wiley-VCH Verlag GmbH & Co. KGaA: **2015**, p 89-124.
6. J. C. G. Bünzli, Rising stars in science and technology : Luminescent lanthanide materials. *Eur. J. Inorg. Chem.* 2017, 5058-5063.
7. J. C. G. Bünzli, On the design of highly luminescent lanthanide complexes. *Coord. Chem. Rev.* 2015, **293-294**, 19-47.
8. K. Bernot; C. Daiguebonne; G. Calvez; Y. Suffren; O. Guillou, A Journey in Lanthanide Coordination Chemistry: From Evaporable Dimers to Magnetic Materials and Luminescent Devices. *Accounts Chem. Res.* 2021, **54**, 427-440.
9. R. G. Pearson, Hard and soft acids and bases - the evolution of a chemical concept. *Coord. Chem. Rev.* 1990, **100**, 403-425.
10. D. G. Karraker, Coordination of trivalent lanthanide ions. *J. Chem. Educ.* 1970, **47**, 424-430.
11. O. Guillou; C. Daiguebonne, Lanthanide ions containing coordination polymers. In *Handbook on the Physics and Chemistry of Rare Earths (vol 34)*, Gschneider, K. A.; Bünzli, J. C. G.; Pecharsky, V. K., Eds. Elsevier: Amsterdam, **2005**; Vol. 34, p 359-404.
12. R. Janicki; A. Mondry; P. Starynowicz, Carboxylates of rare earth elements. *Coord. Chem. Rev.* 2017, **340**, 98-133.
13. T. M. Reneike; M. Eddaoudi; M. Fehr; D. Kelley; O. M. Yaghi, From Condensed Lanthanide Coordination Solids to Microporous Frameworks Having Accessible Metal sites. *J. Am. Chem. Soc.* 1999, **121**, 1651-1657.
14. F. Le Natur; G. Calvez; S. Freslon; C. Daiguebonne; K. Bernot; O. Guillou, Extending the lanthanide terephthalate system : isolation of an unprecedented Tb(III)-based coordination polymer with high potential porosity and luminescence properties. *J. Mol. Struct.* 2015, **1086**, 34-42.
15. O. Guillou; C. Daiguebonne; G. Calvez; K. Bernot, A long journey in lanthanide chemistry : from fundamental crystallogenes studies to commercial anti-counterfeiting taggants. *Accounts Chem. Res.* 2016, **49**, 844-856.
16. C. Daiguebonne; Y. Gérault; O. Guillou; A. Lecerf; K. Boubekeur; P. Batail; M. Kahn; O. Kahn, A new honeycomb-like molecular compound : $\text{Gd}[\text{C}_6\text{H}_3(\text{COO})_3](\text{H}_2\text{O})_3 \cdot 1.5\text{H}_2\text{O}$. *J. Alloys Compd.* 1998, **275-277**, 50-53.
17. X. Fan; S. Freslon; C. Daiguebonne; L. Le Polles; G. Calvez; K. Bernot; O. Guillou, A family of lanthanide based coordination polymers with boronic acid as ligand. *Inorg. Chem.* 2015, **54**, 5534-5546.
18. N. Kerbellec; C. Daiguebonne; K. Bernot; O. Guillou; X. Le Guillou, New lanthanide based coordination polymers with high potential porosity. *J. Alloys Compd.* 2008, **451**, 377-383.
19. N. Rosi; J. Kim; M. Eddaoudi; B. Chen; M. O'Keeffe; O. M. Yaghi, Rod Packings and Metal Organic Frameworks Constructed from Rod-Shaped secondary Building Units. *J. Am. Chem. Soc.* 2005, **127**, 1504-1518.
20. P. D. C. Dietzel; R. Blom; H. Fjellvag, Coordination Polymers Based on the 2,5Dihydroxyterephthalate Ion and Alkaline Earth Metal (Ca, Sr) and Manganese Cations. *Z. Anorg. Allg. Chem.* 2009, **635**, 1953-1958.
21. P. D. C. Dietzel; R. E. Johnsen; R. Blom; H. Fjellvag, Structural Changes and Coordinatively Unsaturated Metal Atoms on Dehydration of Honeycomb Analogous Microporous Metal–Organic Frameworks. *Chem. - Eur. J.* 2008, **14**, 2389-2397.

22. P. D. C. Dietzel; B. Panella; M. Hirscher; R. Blom; H. Fjellvag, Hydrogen adsorption in a nickel based coordination polymer with open metal sites in the cylindrical cavities of the desolvated framework. *Chem. Comm.* 2006, 959-961.
23. P. D. C. Dietzel; Y. Morita; R. Blom; H. Fjellvag, An In Situ High-Temperature Single-Crystal Investigation of a Dehydrated Metal–Organic Framework Compound and Field-Induced Magnetization of One-Dimensional Metal–Oxygen Chains. *Angew. Chem. Int. Ed.* 2005, **44**, 6354-6358.
24. K. Jayaramulu; P. Kanoo; S. J. George; T. K. Maji, Tunable emission from a porous metal–organic framework by employing an excited-state intramolecular proton transfer responsive ligand. *Chem. Comm.* 2010, **46**, 7906-7908.
25. T. Dévic; P. Horcajada; C. Serre; F. Salles; G. Maurin; B. Moulin; D. Heurtaux; G. Clet; A. Vimont; J.-M. Grenèche; B. Le Ouay; F. Moreau; E. Magnier; Y. Filinchuk; J. Marrot; J.-C. Lavalley; M. Daturi; G. Férey, Functionalization in Flexible Porous Solids: Effects on the Pore Opening and the Host-Guest Interactions. *J. Am. Chem. Soc.* 2010, **132**, 1127-1136.
26. Q. Gao; F.-L. Jiang; M.-Y. Wu; Y.-G. Huang; W. Wei; Q.-F. Zhang; M.-C. Hong, Crystal Structures, Topological Analyses, and Magnetic Properties of Manganese-Dihydroxyterephthalate Complexes. *Australian Journal of Chemistry* 2010, **63**, 286-292.
27. Y.-L. Wang; Y.-L. Jiang; Z.-J. Xiahou; J.-H. Fu; Q.-Y. Liu, Diversity of lanthanide(III)-2,5-dihydroxy-1,4-benzenedicarboxylate extended frameworks: syntheses, structures, and magnetic properties. *Dalton Trans.* 2012, **41**, 11428-11437.
28. K. L. Gurunatha; S. Mohapatra; P. A. Suchetan; T. K. Maji, Single-Crystal-to-Single-Crystal Structural Transformation in a Flexible Porous Gadolinium-Organic Framework with Selective and Controlled Sorption Properties. *Cryst. Growth Des.* 2009, **9**, 3844-3847.
29. S. L. Anderson; A. Gladysiak; P. G. Boyd; C. P. Ireland; P. Miéville; D. Tiana; B. Vlasisvljevich; P. Schouwink; W. van Beek; K. J. Gagnon; B. Smit; K. C. Stylianou, Formation pathways of metal–organic frameworks proceeding through partial dissolution of the metastable phase. *Cryst. Eng. Comm.* 2017, **19**, 3407-3413.
30. Y. L. Wang; Y. L. Jiang; Q. Y. Liu; Y. X. Tan; J. J. Wei; J. Zhang, series of three-dimensional lanthanide(III) coordination polymers of 2,5-dihydroxy-1,4-benzenedicarboxylic acid based on dinuclear lanthanide units. *Cryst. Eng. Comm.* 2011, **13**, 4981-4987.
31. J. F. Desreux, In *Lanthanide Probes in Life, Chemical and Earth Sciences*, Choppin, G. R.; Bünzli, J. C. G., Eds. Elsevier: Amsterdam, **1989**; Vol. Elsevier, p 43.
32. H. K. Henisch, *Crystals in Gels and Liesegang Rings*. Cambridge University Press: Cambridge, **1988**.
33. H. K. Henisch; R. Rustum, *Crystal Growth in Gels*. The Pennsylvania State University Press: **1970**, p 1-196.
34. C. Daguebonne; A. Deluzet; M. Camara; K. Boubekour; N. Audebrand; Y. Gérault; C. Baux; O. Guillou, Lanthanide-based molecular materials : gel medium induced polymorphism. *Cryst. Growth Des.* 2003, **3**, 1015-1020.
35. W. Kraus; G. Nolze, POWDER CELL - A program for the representation and manipulation of crystal structures and calculation of the resulting X-ray powder patterns. *J. Appl. Crystallogr.* 1996, **29**, 301-303.
36. T. Roisnel; J. Rodriguez-Carjaval, A Window Tool for Powder Diffraction Patterns Analysis. *J. Mater. Sci. Forum* 2001, **378**, 118-123.
37. T. Roisnel; J. Rodriguez-Carjaval, WinPLOT : a windows tool for powder diffraction pattern analysis. *Materials Science Forum, Proceedings of the Seventh European Powder Diffraction Conference (EPDIC 7)* 2000, 118-123.
38. A. Altomare; M. C. Burla; M. Camalli; G. Cascarano; C. Giacovazzo; A. Guagliardi; A. G. G. Moliterni; G. Polidori; R. Spagna, SIR97: a new tool for crystal structure determination and refinement *J. Appl. Crystallogr.* 1999, **32**, 115-119.
39. G. M. Sheldrick; T. R. Schneider, SHELXL : High-Resolution Refinement. *Macromol. Crystallogr. B* 1997, 319-343.
40. G. M. Sheldrick, A short history of SHELX. *Acta Crystallogr. A* 2008, **64**, 112-122.

41. L. J. Farrugia, WinGX and ORTEP for Windows: an update. *J. Appl. Crystallogr.* 2012, **45**, 849-854.
42. L. J. Farrugia, WinGX suite for smallmolecule single-crystal crystallography. *J. Appl. Crystallogr.* 1999, **32**, 837-838.
43. R. H. Blessing, An empirical correction for absorption anisotropy. *Acta Crystallogr.* 1995, **A51**, 33-38.
44. V. Haquin; M. Etienne; C. Daiguebonne; S. Freslon; G. Calvez; K. Bernot; L. Le Polles; S. E. Ashbrook; M. R. Mitchell; J. C. G. Bünzli; O. Guillou, Color and brightness tuning in hetero-nuclear lanthanide terephthalate coordination polymers. *Eur. J. Inorg. Chem.* 2013, 3464-3476.
45. Y. Luo; G. Calvez; S. Freslon; K. Bernot; C. Daiguebonne; O. Guillou, Lanthanide amino-isophthalate coordination polymers. A promising system for tunable luminescent properties. *Eur. J. Inorg. Chem.* 2011, 3705-3716.
46. J. Wang; Y. Suffren; C. Daiguebonne; K. Bernot; G. Calvez; S. Freslon; O. Guillou, Lanthanide-based molecular alloys with hydroxyterephthalate: a versatile system. *CrystEngComm* 2021, **23**, 100-118.
47. S. I. Weissman, Intramolecular energy transfer - The fluorescence of complexes of europium. *J. Chem Phys* 1942, **10**, 214-217.
48. W. T. Carnall; P. R. Fields; B. G. Wybourne, Spectral intensities of the trivalent lanthanides and actinides in solution. I. Pr³⁺, Nd³⁺, Er³⁺, Tm³⁺ and Yb³⁺. *J. Chem. Phys.* 1965, **42**, 3797-3806.
49. J. C. G. Bünzli; S. V. Eliseeva, Basics of lanthanide photophysics. In *Lanthanide Luminescence*, Hänninen, P.; Härmä, H., Eds. Springer Berlin Heidelberg: 2010, **7**, 1-45.
50. W. T. Carnall; P. R. Fields; K. Rajnak, Spectral intensities of the trivalent lanthanides and actinides in solution. II. Pm³⁺, Sm³⁺, Eu³⁺, Gd³⁺, Tb³⁺, Dy³⁺ and Ho³⁺. *J. Chem. Phys.* 1968, **49**, 4412-4423.

TABLE OF CONTENT



Nd-based and the Yb-based coordination polymers with 2,5-dihydroxyterephthalate (dhbdc²⁻) as ligand exhibit luminescence properties in the near-infrared region.